

ORIGINAL ARTICLE

SLC52A3, A Brown–Vialletto–van Laere syndrome candidate gene is essential for mouse development, but dispensable for motor neuron differentiation

Atsushi Intoh¹, Naoki Suzuki¹, Kathryn Koszka¹ and Kevin Eggan^{1,2,*}

¹Department of Stem Cell and Regenerative Biology, The Harvard Stem Cell Institute, Harvard University, Sherman Fairchild Building, 7 Divinity Avenue, Cambridge, MA 02138, USA and ²The Stanley Center for Psychiatric Research, Broad Institute of Harvard and MIT, Cambridge, MA 02142, USA

*To whom correspondence should be addressed at: Department of Stem Cell and Regenerative Biology, The Harvard Stem Cell Institute, Harvard University, Sherman Fairchild Building, 7 Divinity Avenue, Cambridge, MA 02138, USA. Tel: +1 6174965611; Fax: +1 6173848234; Email: eggan@mcb.harvard.edu

Abstract

Riboflavin, also known as vitamin B2, is essential for cellular reduction-oxidation reactions, but is not readily synthesized by mammalian cells. It has been proposed that riboflavin absorption occurs through solute carrier family 52 members (SLC52) A1, A2 and A3. These transporters are also candidate genes for the childhood onset-neural degenerative syndrome Brown–Vialletto–Van Laere (BVVL). Although riboflavin is an essential nutrient, why mutations in its transporters result in a neural cell-specific disorder remains unclear. Here, we provide evidence that *Slc52a3* is the mouse ortholog of *SLC52A3* and show that *Slc52a3* deficiency results in early embryonic lethality. Loss of mutant embryos was associated with both defects in placental formation and increased rates of apoptosis in embryonic cells. In contrast, *Slc52a3* $-/-$ embryonic stem cell lines could be readily established and differentiated into motor neurons, suggesting that this transporter is dispensable for neural differentiation and short-term maintenance. Consistent with this finding, examination of *Slc52a3* gene products in adult tissues revealed expression in the testis and intestine but little or none in the brain and spinal cord. Our results suggest that BVVL patients with *SCL52A3* mutations may be good candidates for riboflavin replacement therapy and suggests that either the mutations these individuals carry are hypomorphic, or that in these cases alternative transporters act during human embryogenesis to allow full-term development.

Introduction

Riboflavin and its derivatives flavin adenine dinucleotide (FAD) and flavin mononucleotide act as essential cofactors for a variety of metabolic processes, including the electron transport chain. Because riboflavin cannot be readily synthesized in mammalian cells, it must be absorbed from the diet via riboflavin transporters, which have recently been identified in human and rat (1–3). As a result, riboflavin deficient diets have been associated with a variety of developmental and growth disorders (4).

Brown–Vialletto–Van Laere (BVVL) syndrome is a rare neurodegenerative disease characterized by progressive ponto-bulbar

palsy, bilateral sensorineural hearing loss, muscle weakness and amyotrophy (5–8). Respiratory failure as a result of diaphragm denervation is a main cause of death. The origins of this disorder are poorly understood and discovery of genetic variants contributing to this disorder has been slowed by the death of patients prior to reproductive age and its low incidence (9). However, exome sequencing of BVVL patients has recently shown that a subset of patients may be homozygous for rare coding variants in *C20ORF54* (9–16). *C20ORF54* encodes *SLC52A3*, one of the three recently identified candidate riboflavin transporters, which share considerable homology. Subsequent exome and candidate gene

Received: January 8, 2016. Revised: January 8, 2016. Accepted: February 15, 2016

© The Author 2016. Published by Oxford University Press. All rights reserved. For Permissions, please email: journals.permissions@oup.com

sequencing studies have further implicated this class of transporters in BVVL, showing that distinct patients can harbor rare variants in another riboflavin transporter gene, *SLC52A2* (10,16–18). Thus far, *SLC52A1* mutations have yet to be seen in BVVL patients. These discoveries have led to reported attempts to administer riboflavin to children with BVVL, with some reports of anecdotal improvement in their condition (19).

However, it remains untested whether there is a causal relationship between mutations in the class of putative riboflavin transporters and neural degeneration in BVVL. Furthermore, it is unknown in which cell types each of these putative transporters acts to allow the movement of riboflavin or other substrates. Addressing these questions experimentally might allow the validity of riboflavin replacement therapy in BVVL to be modeled and provide insight into the optimal route of administration.

Here, we show that *Slc52a3* is the mouse ortholog of *C20ORF54* (*SLC52A3*) and that a homozygous disruption of this locus results in early embryonic lethality. Although mutant embryos did not survive beyond mid-gestation, we were able to generate homozygous mutant embryonic stem (ES) cells and found that they could be readily differentiated into motor neurons. Consistent with this observation, we found that *Slc52a3* was most strongly expressed in the intestine, placenta as well as the testis, but was largely absent from the adult brain, an expression pattern mirrored by its human ortholog, *C20ORF54* (*SLC52A3*). In total, our studies in the mouse suggest *Slc52a3* functions during early development and in the intestine based on the protein expression profile, making BVVL patients with *SLC52A3* mutations interesting candidates for riboflavin replacement therapy.

Results

SLC52A2 and 3 but not 1 conserved in mouse

Three putative riboflavin transporters have been identified in human and are encoded by three independent but homologous genes (*SLC52A1*, *SLC52A2* and *SLC52A3*) (2,3,20,21). At the protein level, *SLC52A1* and *SLC52A2* are the most conserved displaying >87% sequence similarity, while *SLC52A3* shows more divergence with 44% overlap to *SLC52A1*, and 43% conservation with *SLC52A2* (Fig. 1A). In contrast, the rat and mouse genomes only appear to carry two genes with similarity to this family of transporters, with the mouse *SLC52A2* protein showing 80% identity to human *SLC52A2* and mouse *Slc52a3* showing >74% identity to human *SLC52A3* (Fig. 1A and B and Supplementary Material, Fig. S1A). In contrast, we could find no gene with conserved homology to *SLC52A1* in the syntenic portion of the mouse genome: orthologs of human genes surrounding *SLC52A1* on human chromosome 17 were found on mouse chromosome 11 in similar positions and orientations (Supplementary Material, Fig. S1B). At the site where the mouse ortholog of *SLC52A1* might be expected to be found there were instead an apparent lincRNA-encoding gene (*Gm12320*) and an unstudied protein-coding gene (*Gm12318*), with no homology to *SLC52A* family members. Further searches for genes with homology to *SLC52A* members in the mouse genome also failed to locate an *SLC52A1* mouse ortholog. We, therefore, conclude that while humans have three *SLC52A* family members, mice appear to contain only two.

The human *SLC52A3* protein is well conserved between vertebrates and has 11 predicted integral membrane regions, which likely function to transport riboflavin across biological membranes (Fig. 1A, Supplementary Material, Fig. S1C). Alignment comparison of presumptive *SLC52A3* protein sequences between all vertebrates in NCBI BLAST showed that BVVL patient

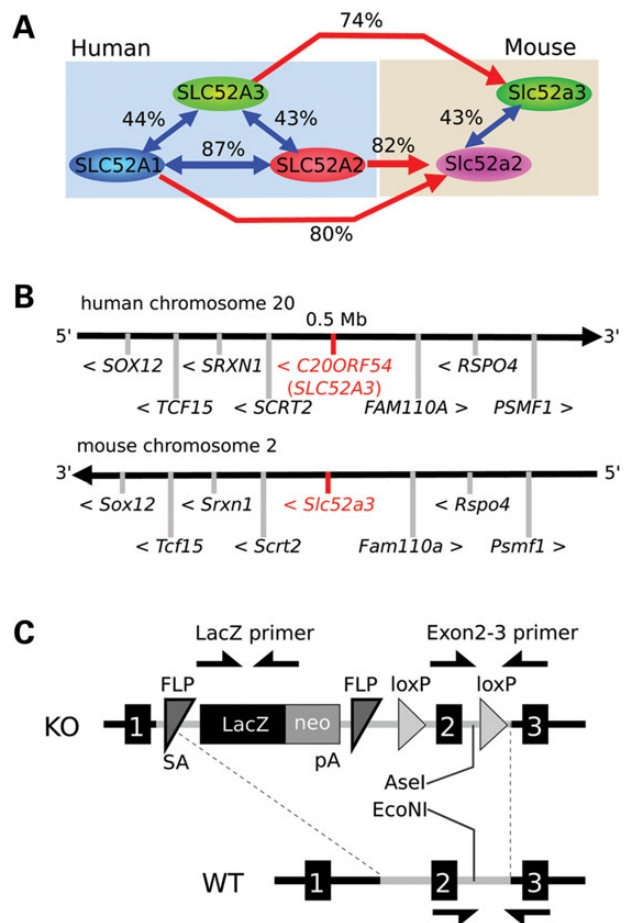


Figure 1. Gene information of riboflavin transporters, the target genes in BVVL syndromes. (A) Riboflavin transporter members in human and mouse. Human and the other primates have three members; *SLC52A1*, *SLC52A2* and *SLC52A3*, though rodents have two; *Slc52a2* and *Slc52a3*. Each transporter has high homologies between human and mouse. Similarity of *SLC52A3* with *SLC52A1* and 2 is lower (<50%). No homolog of *SLC52A1* exists in mouse, but human *SLC52A1* has high similarity with human *SLC52A2*, suggesting *SLC52A1* is a duplicated gene from *SLC52A2*. Similarity values between these proteins were calculated by NCBI BLAST. (B) Comparing human and mouse riboflavin transporter gene: *SLC52A3* and the surrounding genes. The genes surrounding human and mouse *SLC52A3* are highly conserved between human chromosome 20 and mouse chromosome 2, suggesting those genes are definitely homolog genes. (C) Gene schema of *Slc52a3* knock-out mouse. Genotyping was performed with primers against LacZ and Exons 2 and 3 (arrows). After amplifying Exons 2 and 3 region by PCR, restriction enzyme digests with AseI and EcoNI was performed. In homozygous mutant mice, PCR products with Exons 1 and 2 primer sets are digested with AseI, but undigested with EcoNI. PCR products from WT are digested with EcoNI only. DNA fragments from PCR products of heterozygous mutant mice are found in both AseI and EcoNI digestion.

mutations were biased to highly conserved regions of the protein (Supplementary Material, Figs S1D and S2). These mutant residues were also highly conserved in the distinct human transporters *SLC52A1* and *SLC52A2*, suggesting these regions may be critical for correct protein folding or riboflavin transport activity (Supplementary Material, Fig. S2).

Slc52a3 knock-out is embryonic lethal

In order to investigate the function of *Slc52a3* in a mouse model, we obtained mutant embryos harboring a targeted insertion

Table 1. Genotyping frequency in each embryo stage and after wean (3 weeks old).

| Stage | -/- | +/- | WT | Total | P | c2 |
|------------|-----|-----|----|-------|-------------|-------|
| After wean | 0 | 117 | 57 | 174 | 2.50019E-13 | - |
| E10.5 | 2 | 22 | 11 | 35 | 0.0310 | 6.943 |
| E9.0 | 7 | 35 | 19 | 61 | 0.0486 | 6.049 |
| ESC | 6 | 10 | 4 | 20 | 0.8187 | 0.4 |

P: possibilities calculated by χ^2 tests (C2).

between Exons 1 and 2 from the knock-out mouse project (KOMP) consortium (17). This insertion contained a *LacZ* reporter and transcriptional terminator downstream of a strong splice-acceptor. Thus, this allele would be predicted to serve as both a transcriptional reporter of *Slc52a3* activity and a loss of function mutation (Fig. 1C). After transfer of frozen embryos to recipient females, we obtained candidate *Slc52a3* +/- heterozygous mutant mice. We observed no genotype dependent change in weight over the first 24 weeks of their life ($n = 11$ mice for each genotype) or other overt phenotypes in these animals over 2 years of maintenance ($n = 6$ mice of each genotype) (Supplementary Material, Fig. S3A). As children diagnosed with BVVL were found to carry independent rare variants in each of their two alleles of *SLC52A3*, we next attempted to produce homozygous mutant animals. However, extensive intercrossing between heterozygotes failed to generate homozygous *Slc52a3* mutant animals and instead produced only +/- and WT animals in a 2:1 ratio ($n = 174$ pups) (Table 1). Although our genotyping strategy could in principle clearly distinguish between heterozygous and homozygous mutants (Supplementary Material, Fig. S3B), the substantial number of crosses we performed also allowed us to statistically demonstrate that it was unlikely homozygous mutants were hidden in our heterozygous class of animals ($P < 0.05$, Table 1). Thus, we concluded that in the mouse, *Slc52a3* loss of function results in embryonic lethality. To determine when *Slc52a3* became essential, we further analyzed embryos from *Slc52a3* +/- crosses at several early developmental stages.

Slc52a3 mutants lost at mid-gestation

We found that we could readily recover homozygous mutant embryos at 9.5 dpc and that although they were recovered at slightly less than expected frequency, they seemed to have no overt phenotypes (Fig. 2A and B). By Day 10.5, the frequency of mutants became even further skewed from expected ratios and those embryos that were recovered displayed abnormal morphologies (Table 1 and Fig. 2C and D). Staining with antibodies specific to the apoptotic indicator terminal deoxynucleotidyl transferase dUTP nick end labeling (TUNEL) also demonstrated a significant increase in the number of apoptotic cells in E10.5 mutants relative to controls (Fig. 2E and F).

Establishment of *Slc52a3* knock-out ES cells

To attempt to create homozygous mutant cells for validation of the loss-of-function effects of the *Slc52a3* allele we studied in embryos, we attempted to produce *Slc52a3* mutant ES cell lines. After intercrossing heterozygous animals, we harvested blastocysts, then cultivated inner cell mass outgrowths under standard (2i) growth condition (22,23) (Fig. 3A). We found that we could generate ES cell lines of each of the expected three genotypes at the expected Mendelian ratios (Table 1 and Fig. 3B). These cells expressed pluripotency markers such as Oct-3/4 and Sox2

(Fig. 3C). Western blotting analysis demonstrated the expression of *Slc52a3* in heterozygous and WT ES cells. However, the levels of *Slc52a3* in -/- mutant ES cells was significantly reduced with <3% of the normal protein level remaining in homozygous mutant cells (Fig. 3C-E). Interestingly, we noted that *Slc52a3* -/- ES cells exhibited a modest but significant decrease in the expression of Oct3/4 (Fig. 5B). However, we did not note any change in the morphology and growth characteristics of mutant ES cells, nor did we note any overt change in the expression of indicators of pluripotency as assessed by immuno-staining (Fig. 3C). Thus, we conclude that while embryonic development seemed highly sensitive to depletion of *Slc52a3*, normal level of this protein were not essential for development to the blastocyst stage or normal ES cell growth and maintenance.

Slc52a3 knock-out causes placental deficiency

To further investigate potential causes for the embryonic loss of -/- mutants we examined the expression pattern of *Slc52a3* in the developing embryo. X-gal staining of +/- embryos suggested that *Slc52a3* was expressed in the placenta at E10.5 (Fig. 4A). Western blotting confirmed that the *Slc52a3* protein was expressed in the placenta of control embryos (Fig. 4B). Immunofluorescent staining of dissected embryos suggested minimal expression of *Slc52a3* in fetal tissues at E8.5 and E10.5. In contrast, we observed strong staining in extraembryonic tissues at both Days 8.5 (Fig. 4C) and 10.5 (Fig. 4D). Based on our finding that *Slc52a3* seemed to be predominantly expressed in extraembryonic tissues, we isolated E10.5 conceptuses and histologically examined their developing placentas. We found *Slc52a3* -/- embryos lost most of their placental tissues by Day 10.5 (Fig. 4E). We could confirm the presence of decidual, giant cell, and placental labyrinth tissues in the extra embryonic field of WT embryos. However, homozygous mutant embryos maintained only the giant cell layer between the decidua and yolk sac, and had lost the placental labyrinth.

Motor neuron differentiation of *Slc52a3* mutant ES cells

Because BVVL syndrome is a neurodegenerative disease with upper and lower motor neuropathy (5-8), the loss of homozygous mutant embryos early in development precluded us from addressing whether or not *Slc52a3* has an important function in the normal development or short-term survival of motor neurons in the spinal cord. To address this issue, which has important implications for the role mutations in this gene might play in BVVL patients, we differentiated mouse ES cell lines with +/+, +/- and -/- genotypes into motor neurons using a well-established method (24). To quantify the efficiency of motor neuron differentiation and persistence in culture we measured the expression of ISL transcription factors, which are expressed in many motor neuron subtypes (24). Examination of the relative abundance of *Isl1* transcripts by reverse transcriptase-polymerase chain reaction (RT-PCR) suggested that there was no statistically significant difference between mutant and control cultures at either 7 or 14 days of motor neuron differentiation (Fig. 5A-C). Quantification of the number of presumptive motor neurons expressing both Tuj1 and *Isl1/2* after 14 days of differentiation of the three genotypes of stem cell lines also indicated there were no overt changes in the survival of this neuronal sub-type imposed by *Slc52a3* -/- loss of function (Fig. 5D and E). To provide further insight into whether *Slc52a3* plays an important role in motor neuron biology, we also monitored its expression during directed differentiation into this cell type. Strikingly, we found that *Slc52a3* expression

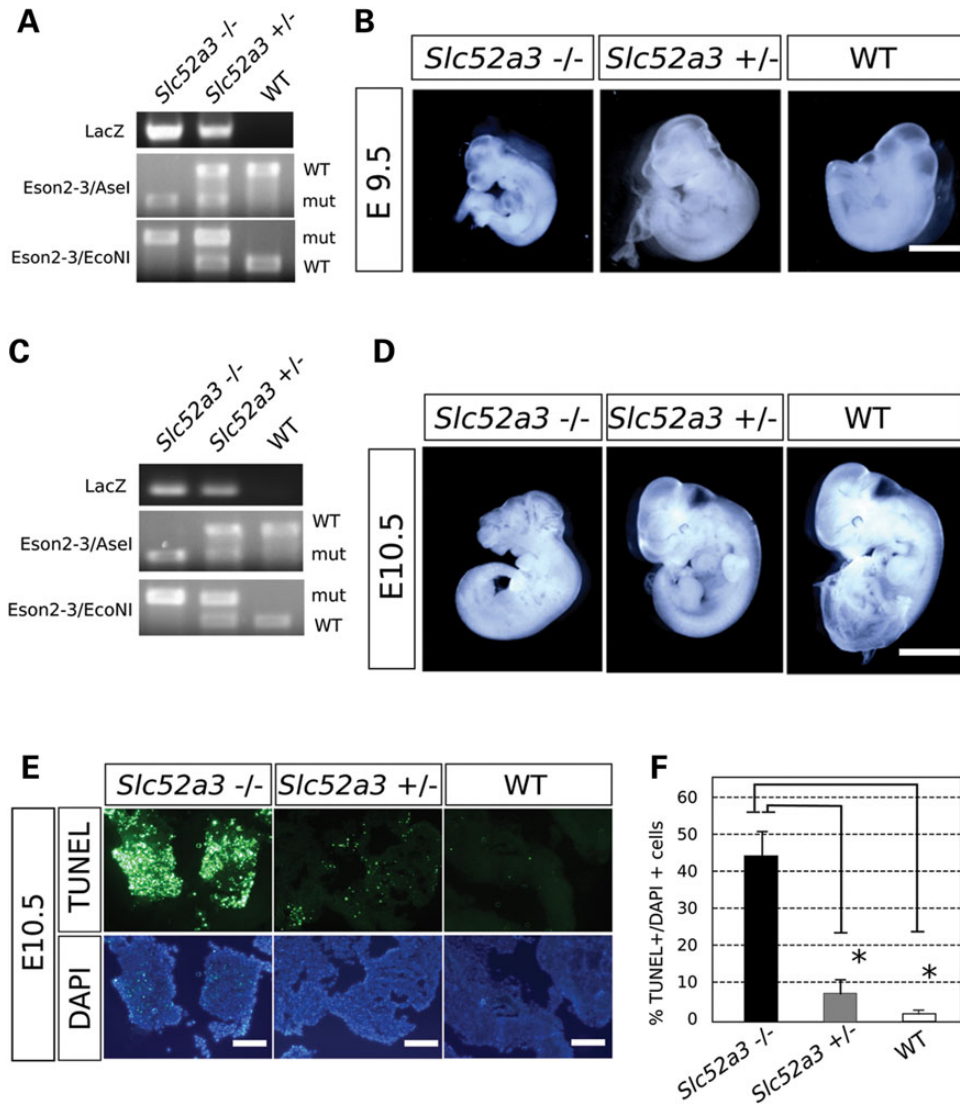


Figure 2. *Slc52a3* KO mouse is embryonic lethal. (A and B) Day 9.5 embryos resulting from heterozygous mutant mice crossing. (A) Genotyping PCR results. (B) Recovered embryos of each genotype. Bar, 300 μ m. (C and D) Day 10.5 embryos resulting from heterozygous mutant mouse crossing. (C) Genotyping PCR results. (D) Recovered embryos of each genotype. Homozygous KO embryos have severe developmental abnormality. Bar, 1 mm. (E) TUNEL assay in E10.5 embryos of each genotype. Bars: 100 μ m. (F) Ratio of TUNEL positive cells to DAPI positive cells. ** $P < 0.01$.

was significantly and dramatically reduced after 7 days of differentiation and essentially absent at 14 days when compared with ES cell levels (Fig. 5A). We, therefore conclude *Slc52a3* is unlikely to play an important role in the initial development of spinal motor neurons.

Slc52a3 expression in adult tissues

Although we could not readily assess whether *Slc52a3* serves an important postnatal function due to the loss of mutant embryos, we examined its expression pattern in adult animals to determine whether the resulting information might provide further insight into how mutations in this gene could contribute to the phenotype of individuals with BVVL. A broad survey of the relative expression of *Slc52a3* by quantitative RT-PCR indicated that transcripts were present in intestine and testis, but absent or rare in the brain, spinal cord, heart, lung, liver and musculature (Fig. 6A). Western blotting demonstrated the presence of *Slc52a3* protein in the intestine, seminal vesicles and testes as well as its apparent absence in

the cerebrum (Fig. 6B). Immuno-staining and X-gal staining confirmed expression in intestine and the male reproductive organs (Fig. 6C–E). We found *Slc52a3* was expressed in the intestinal villus (Fig. 6C), suggesting *Slc52a3* may play a role in the absorption of riboflavin from the diet. Examination of the testis indicated strong expression of *Slc52a3* in the stromal Leydig cells, but not in seminiferous tubules themselves, where sperm maturation occurs (Fig. 6D). In the seminal vesicle, where mature sperm accumulate, we observed *Slc52a3* expression in epithelial cells (Fig. 6E).

Expression of riboflavin transporter family in human and mouse tissues

We next sought to reconcile our observations in *Slc52a3* mutant mice with the pathology observed in BVVL patients harboring *SLC52A3* mutations by mining and examining the expression pattern of the human gene in existing expression databases (Supplementary Material, Fig. S4). By examining data from BioGPS (<http://biogps.gnfn.org/>), we found that similar to the situation in mouse,

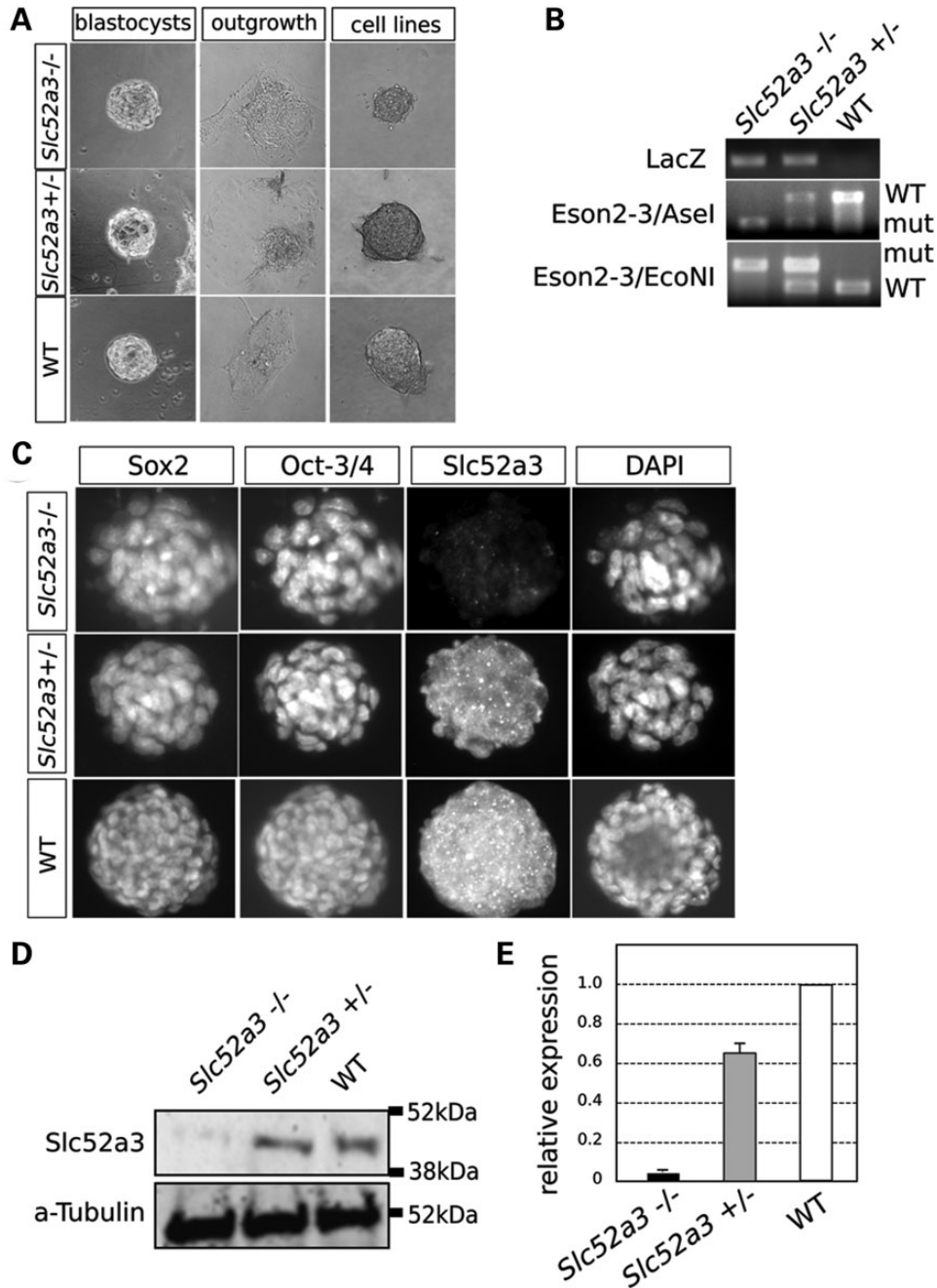


Figure 3. Establishment of *Slc52a3* KO ES cells. (A) Day 4.5 embryos (blastocysts) from heterozygous crossing were harvested and cultured in ES media with 2i/LIF (left panels). Five-day-culture of blastocysts led the outgrowth of the inner cell mass (middle panels). Outgrowing cell colonies in 2i/LIF condition on gelatin-coated dish were picked and cell lines were established (right panels). The total number of the established cell lines and the genotype ratio are shown shown in Table 1. (B) Genotyping results of the established ES cells. (C) Established cell lines stained with anti-pluripotent markers; Sox2 and Oct-3/4 and anti-*Slc52a3* in each genotype. *Slc52a3*^{-/-} cell lines have limited expression of the target gene even though expression of the pluripotent markers seems to be normal. (D and E) Western blotting of pluripotent ES cell lysates. Relative expression levels were normalized by α -tubulin expression.

human *SLC52A3* transcript was present in the intestine, testis and placenta. However, we also noted that *SLC52A1*, the candidate transporter not present in the mouse genome was also expressed in the human placenta as well the digestive and reproductive tracks (Supplementary Material, Fig. S4). Examination of these data sets independently confirmed our observation that *Slc52A3* expression was largely or completely absent in the nervous system. Instead, *SLC52A2*, which exhibited a broad expression profile, seemed to be the primary candidate riboflavin transporter expressed in the brain.

Discussion

Here, we have shown that a loss-of-function mutation in *Slc52a3* leads to embryo lethality around Day 10.5, potentially due to a failure in placental development (Fig. 4). In the placental labyrinth, a complex vascular structure allows for the exchange of nutrients and oxygen between maternal and fetal blood (Fig. 7A). Our studies indicate that in the absence of *Slc52A3*, the placental labyrinth either does not form properly, or cannot function normally and is not maintained. As a result, it would appear

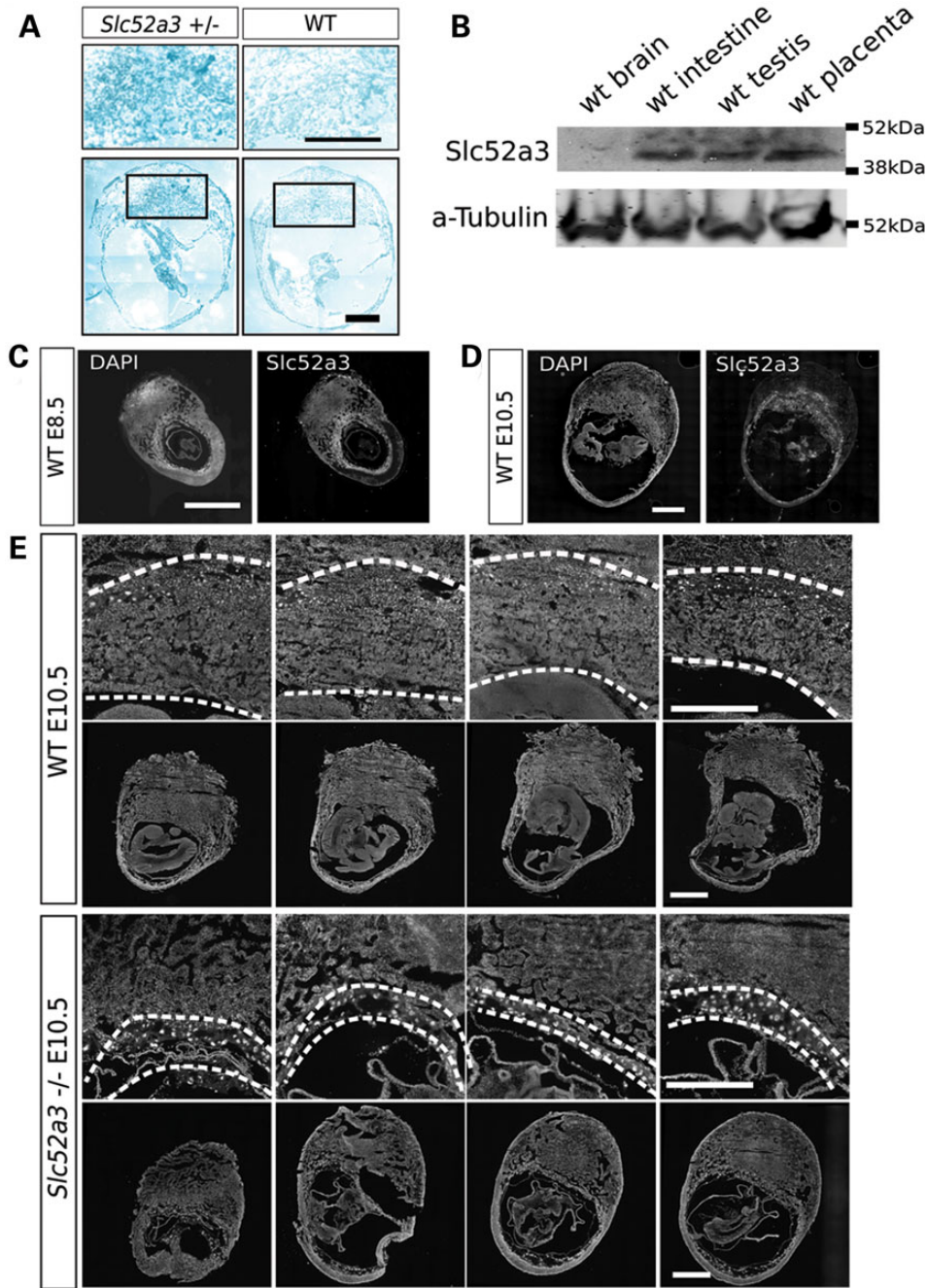


Figure 4. *Slc52a3* KO embryo has placental loss at Day 10.5 extraembryonic tissues. (A) X-gal staining of *Slc52a3* ^{+/-} and WT embryos with extraembryonic tissues at Day 10.5. (B) Western blotting of WT adult tissues and placenta at Day 10.5. (C) Days 8.5 and (D) 10.5 embryos stained with antibodies of *Slc52a3*. (E) Sequential dissections of *Slc52a3* ^{-/-} and WT embryos at Day 10.5 were stained with DAPI. Broken lines show the placental regions from giant cell layers to amniotic membranes. Bars: 500 μ m.

that the mouse embryo is deprived of not only riboflavin, but also other key maternal factors necessary for survival. Although it is not clear precisely how loss of this transporter impacts extraembryonic development, recent report have shown that one riboflavin derivative, FAD, activates lysine-specific demethylase 1, which can contribute to histone H3-K4 demethylation (25) and therefore changes in cellular behavior.

Our findings provide further insight into the role that candidate causative mutations in *SLC52A* gene family members may play in BVVL (9–16). Although the early loss of mutant embryos precluded a functional test of the hypothesis, our gene expression studies

support the notion that *Slc52A3* plays an important role in absorbing riboflavin in the gut, either to support specific aspects of gut function, or to facilitate uptake of riboflavin into the blood (1,26). In contrast, these data support the view that patient mutations in *SLC52A2*, may influence the function of a much more widely expressed transporter, which is also expressed in the brain (10,16–18).

SLC52A1 was first riboflavin transporter identified in humans and it seems to exist only within the primate lineage (2). No obvious orthologs have been identified in other vertebrates. *SLC52A1* is highly similar to *SLC52A2*, suggesting that *SLC52A1* may have

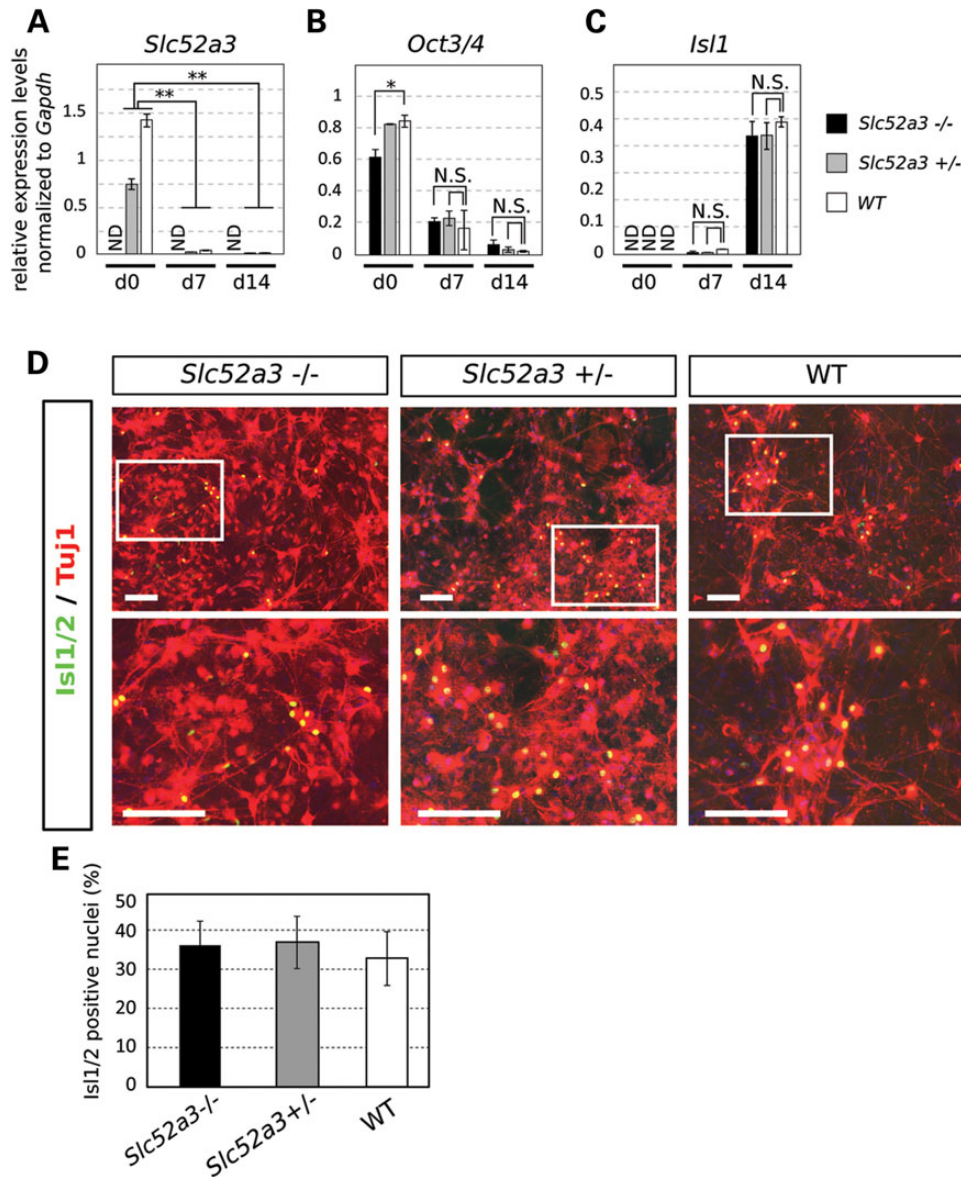


Figure 5. Motor neuron differentiation of *Slc52a3* KO ES cells. (A–C) qPCR assay of *Slc52a3*, *Oct3/4* and *Isl1* were performed through the differentiation into motor neurons at Day 0, 7 and 14. * $P < 0.05$; ** $P < 0.01$, N.S.: no significance, ND: not detected. All expression levels were normalized to GAPDH. (D) Motor neurons derived from ES cells from each genotype were stained with anti-*Isl1/2* / *Tuj1*. (E) Percentage of motor neurons from each culture was determined by quantification of *Isl1/2* / *Tuj1* positive cells. Bars: 200 μ m.

arisen through gene duplication of an ancestral form *SLC52A2* (Fig. 1A and Supplementary Material, Fig. S2). Interestingly, *SLC52A1* is a candidate gene for multiple acyl-CoA dehydrogenation deficiency, which results from riboflavin deficiency in pregnancy (27). Although we found that the loss of *Slc52a3* function resulted in early termination, compound heterozygous carriers of mutations in human *SLC52A3* development, apparently normally, until well into childhood. Our studies combined with patient observations suggest that *SLC52A1* expression may compensate for reduced *SLC52A3* function in those individuals (27).

Although *SLC52A1* and *SLC52A3* are both expressed in the human intestine, BVVL patients with *SLC52A3* mutations have a significant decrease in riboflavin plasma levels (11). Therefore, it may be that failure of riboflavin absorption in the intestine and the resulting short supply in neural tissues might lead to BVVL in such patients (Fig. 7B). Our analysis of the expression pattern of *Slc52a3* in mice suggests it may also play an important role in

intestinal riboflavin transport. Given the early embryonic lethality of *Slc52a3* mutations in the mouse, generation of a conditional mutant allele will be required to test this hypothesis. Nevertheless, the expression pattern of *SLC52A3* and its mouse ortholog support the proposal that supplying riboflavin intravenously to BVVL patients harboring mutations in this gene may bypass the primary site of its activity and provide some therapeutic value.

Materials and Methods

Genomic DNA and total RNA preparation

Genomic DNA was harvested with the Tail Direct PCR kit (Allele Biotechnology) according to the manufacturer's protocol. Total RNA samples were isolated with Trizol (Invitrogen). cDNA samples were reverse transcribed using the iScriptc DNA Synthesis Kit (Bio-Rad) for subsequent qPCR assay with SYBR green qPCR Supermix (Bio-Rad).

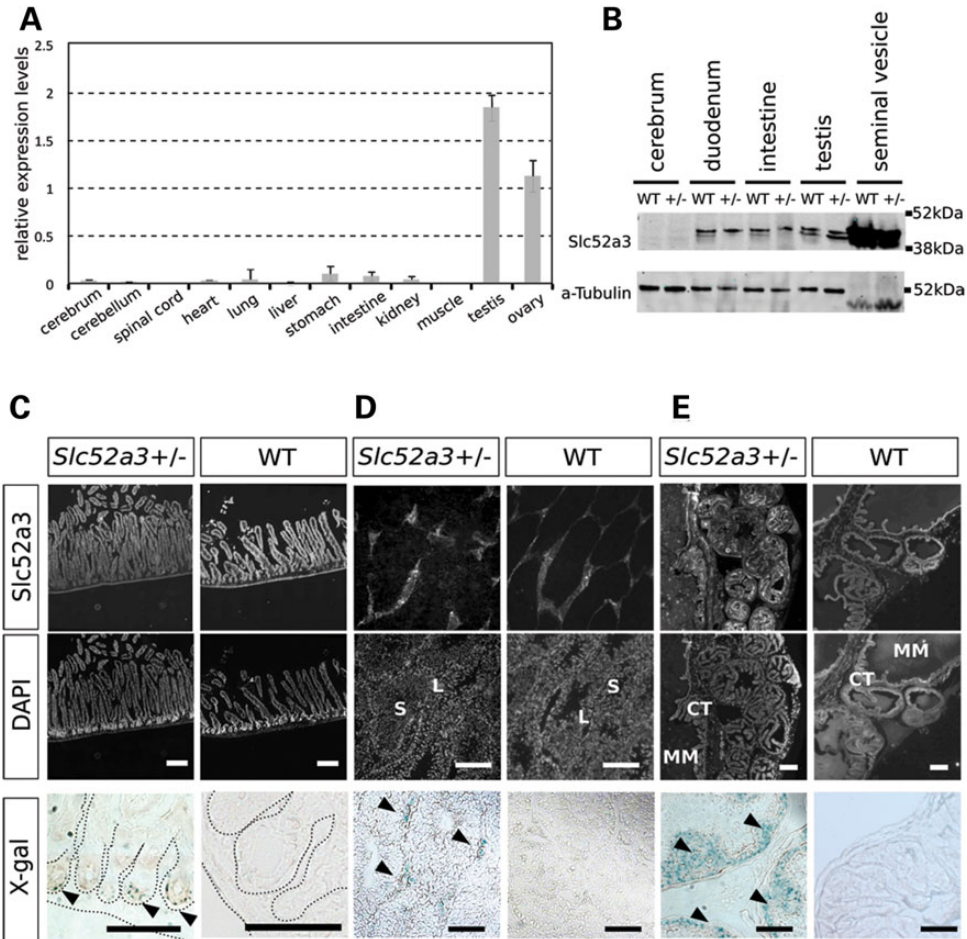


Figure 6. *Slc52a3* expression in adult tissues. (A) qPCR assay of *Slc52a3* expression in adult tissues. Expression levels were normalized by *GAPDH*. (B) Western blotting of adult tissues. (C–E) Immunofluorescent staining and X-gal staining of anti-*Slc52a3* in intestine (C), testis (D) and seminal vesicle (E). V, intestinal villus; IC: intestinal crypt; S, seminiferous tubule; L, Leydig cells; CT, connective tissue; MM, mucous membrane. Bars: 200 μ m.

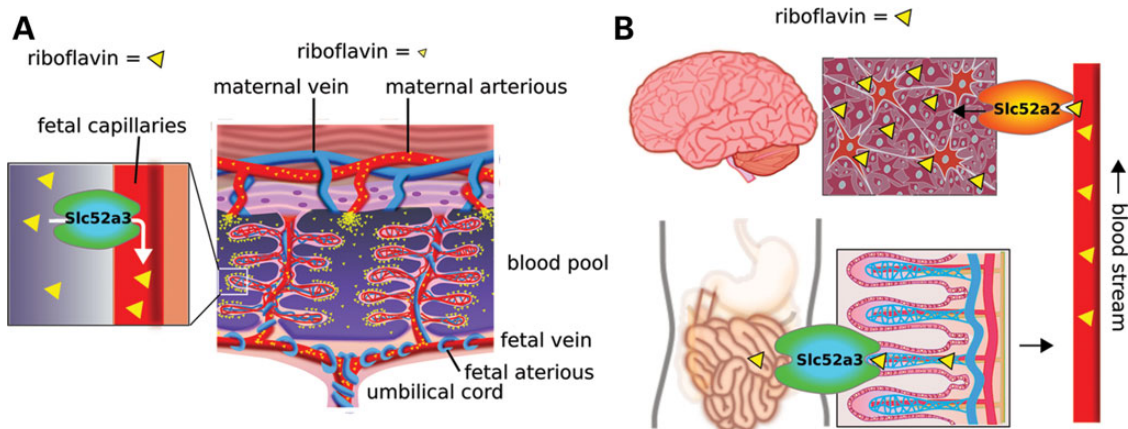


Figure 7. Scheme of the *SLC52A3* function in embryo development and BVVL patients. (A) Mechanism of riboflavin absorption in mouse placenta. Embryo vein absorbs riboflavin from the intervillous blood pool in which maternal blood supplies essential nutrients. Riboflavin is suggested to be absorbed through *Slc52a3* to the fetal vein and supplied to fetus through umbilical cord. (B) A hypothesis of pathogenesis in BVVL syndrome. *SLC52A3* in the intestine and spinal cord. Riboflavin is absorbed in the intestine through *SLC52A3* transport. Riboflavin is expected to be absorbed from the blood stream to neural tissues via *SLC52A2*.

Genotyping PCR

Primer sequences for genotyping are as follows: LacZ forward: 5'- ATCACGACGGCTGTATC, reverse: 5'- ACATCGGGCAAATAA-TATCG; Exons 1 and 2 forward: 5'-CAGGACACCTTGAACACT,

reverse: 5'-AGAAGAGCAGTGGCGAGAAG. Genomic DNA and primers (50 nm each) were mixed with AmpliTaq Gold 360 Master Mix (Thermo Fisher Scientific). Thermal cycling conditions were 5 min at 95°C followed by 35 cycles of 30 s at 95°C, 30 s at 55°C and

1 min at 72°C. After enzymatic amplification for 35 cycles with Exons 1 and 2 primers, the PCR products were digested with the restriction enzyme *AseI* (New England Biolabs, R0526S) and *EcoNI* (New England Biolabs, R0521S) for 3 h at 37°C followed by 10 min at 80°C, and resolved on a 1% agarose gel in Tris acetate-ethylene-diaminetetraacetic acid (EDTA) buffer.

Primers for quantitative PCR

Primer sequences for qPCR are as follows; *mSlc52a3* forward: 5'-CCTGGTACCTGCCTTCTTACC, reverse: 5'-TGTATCCAGGAGGTCACGTTTC, *mOct-3/4* forward: 5'-TCTTTCCACCAGGCCCGGCTC, reverse: 5'-TGCGGGCGGACATGGGGAGATCC; *mIsl1/2* forward: 5'-TATCCAGGGGATGACAGGAAC, reverse: 5'-GCTGTTGGGTGTATCTGGGAG, *mGAPDH* forward: 5'-TTCACCACCATGGA GAAGGC, reverse: 5'-GGCATGGACTGTGGTCATGA.

Antibodies

Antibodies used in this study included anti-C20ORF54 for mouse *Slc52a3* staining (rabbit polyclonal, Santa Cruz, sc85426), anti-mouse Oct-3/4 (mouse monoclonal, Santa Cruz, sc5279), anti-mouse Sox2 (goat polyclonal, Santa Cruz, sc17320), anti-mouse Isl-1/2 (mouse monoclonal IgG1, DSHB, 40.2D6), anti-mouse Tuj1 (mouse monoclonal IgG2a, Covance Antibody Products, MMS-435P) and anti- α -Tubulin (mouse monoclonal, Sigma-Aldrich, T6199). Cell nuclei were stained with the VECTASHIELD Mounting medium with 4',6-diamidino-2-phenylindole (DAPI) (Vector Laboratories, H-1200).

Quantitative polymerase chain reaction

qPCR with SYBR green was performed in triplicate in three independent experiments using CFX96™ Real-Time System (Bio-Rad). The housekeeping gene glyceraldehyde-3-phosphate dehydrogenase, *GAPDH*, was used as an internal control to normalize the expression levels using the $\Delta\Delta C_t$ method for quantification. The thermal cycling conditions were 5 min at 95°C followed by 35 cycles of 30 s at 95°C, 30 s at 55°C and 1 min at 72°C.

Slc52a3 mutant mice

All of the experimental protocols and procedures were approved by the Institutional Animal Care and Use Committee at Harvard University. The *Slc52a3*^{tm2a(KOMP)Wtsi} frozen embryos were purchased from the KOMP, and transferred into foster mothers. Heterozygous mutants were confirmed by genotyping PCR of those pups. Those mutants were crossed and the F1 generations were obtained. The genotype ratio of a total of 174 mice bred by crossing heterozygous mutants was quantified. Using a χ^2 test, statistical analysis was performed by the following equation.

$$\chi^2 = \sum [(O - E)^2 / E]$$

O: observed frequency count, E: expected frequency count (Table 1).

Harvesting mouse embryos

Harvested embryos in each stage were genotyped and fixed in 4% paraformaldehyde (PFA) solution at 4°C overnight for subsequent cryodissection into 20 μ m sections with OCT compound (Tissue Tek). The samples were blocked with 5% Donkey serum (Jackson ImmunoResearch Laboratories) in PBS followed by antibody staining. TUNEL assay was performed on Day 10.5 embryos from

heterozygous mutant crossings. TUNEL staining was performed according to the manufacturer's instructions (Click-iT® TUNEL Alexa Fluor® 488 Imaging Assay, Invitrogen). The genotype ratio of a total of 45 embryos at Days 10.5 and 61 embryos at Day 9.5 resulting from crossing heterozygous mutants was determined. Statistical significance was calculated using a χ^2 test (Table 1).

Establishment of mouse *Slc52a3* KO ES cells

Three-month-old female mice injected with pregnant mare's serum gonadotrophin followed 48 h later by human chorionic gonadotropin were mated. Four days following the crossing date, the pre-implantation embryos were flushed directly from the uterus, and cultured the harvested blastocysts in mouse ES media containing 20% fetal bovine serum, 1% glutamax (GIBCO), 2-mercaptoethanol and 1% penicillin/streptomycin (GIBCO) in the Dulbecco's modified Eagle's medium (DMEM) (GIBCO) with 1 μ M PD0325901, 3 μ M CHIR99021 and 1000 units/ml leukocyte inhibiting factor (LIF) on a gelatin-coated dish. After 5 days, the inner cell masses were picked and cultured in ES media with 2i/LIF to establish ES cell lines. The protein samples in the pluripotent state were prepared in extraction buffer containing 7 M urea, 2 M thio-urea, 0.2% sodium dodecyl sulphate, 20 mM 4-(2-hydroxyethyl)-1-piperazineethanesulfonic acid (pH7.4), 10 mM NaF, 1 mM EDTA, 1 mM dithiothreitol, and proteinase inhibitor cocktail (Complete, Roche). A statistical calculation was performed with genotyped ratio of established cell lines.

Motor neuron differentiation

Mouse ES cells from each genotype were differentiated into motor neurons as described previously (24,28). Briefly, trypsinized ES cells were cultured via EB formation in DMEM-F12 (GIBCO) with 10% knock-out serum (GIBCO), 1% glutamax, 2-mercaptoethanol and 1% penicillin/streptomycin. The EBs were treated with 100 nM retinoic acid and 1 μ M smoothed antagonist from Days 3–7. On Day 7, the EBs were digested into single-cells with papain containing 1000 units/ml DNaseI (Worthington Biochemical). Resuspended cells were plated on Matrigel (FISHER) -coated dish with a concentration of 10 000 cells/ml in the F12 medium (GIBCO) containing 5% horse serum (GIBCO), B-27 supplement and N2 supplement (GIBCO) with 10 ng/ml glial derived neurotrophic factor, ciliary neurotrophic factor and brain derived neurotrophic factor (R&D Systems). Total RNA samples were prepared at Days 7 and 14. For the motor neuron survival experiments, differentiated cells were stained using immunofluorescence at Day 14.

Preparing adult tissues for experiments

Four-month-old mice were anesthetized with avertin and perfusion-fixed with 4% PFA. Tissues were harvested and post-fixed in 4% PFA overnight at 4°C, washed with PBS, immersed in 30% sucrose overnight at 4°C and frozen in OCT compound for sectioning using cryostat. Tissues were also harvested from anesthetized mice without 4% PFA treatment, digested in protein extraction buffer described above, and Trizol to prepare RNA samples, respectively.

X-gal staining

X-gal activity was assessed by incubating 20 μ m thick sections with freshly prepared LacZ staining solution (1.0 mg/ml of X-gal, 4 mM potassium ferrocyanide, 4 mM potassium ferricyanide and 2 mM MgCl₂ in phosphate buffer) overnight at 37°C. The sections were examined and photographed with a Zeiss AX10.

Supplementary Material

Supplementary Material is available at HMG online.

Conflict of Interest statement. None declared.

Funding

This work was supported by the Thisbe and Noah Scott Foundation and the Howard Hughes Medical Institute.

References

- Fujimura, M., Yamamoto, S., Murata, T., Yasujima, T., Inoue, K., Ohta, K.Y. and Yuasa, H. (2010) Functional characteristics of the human ortholog of riboflavin transporter 2 and riboflavin-responsive expression of its rat ortholog in the small intestine indicate its involvement in riboflavin absorption. *J. Nutr.*, **140**, 1722–1727.
- Yonezawa, A., Masuda, S., Katsura, T. and Inui, K. (2008) Identification and functional characterization of a novel human and rat riboflavin transporter, RFT1. *Am. J. Physiol. Cell. Physiol.*, **295**, C632–C641.
- Yao, Y., Yonezawa, A., Yoshimatsu, H., Masuda, S., Katsura, T. and Inui, K. (2010) Identification and comparative functional characterization of a new human riboflavin transporter hRFT3 expressed in the brain. *J. Nutr.*, **140**, 1220–1226.
- Powers, H.J. (2003) Riboflavin (vitamin B-2) and health. *Am. J. Clin. Nutr.*, **77**, 1352–1360.
- BROWN, C.H. (1894) Infantile amyotrophic lateral sclerosis of the family type. *J. Nerv. Ment. Dis.*, **19**, 707–716.
- Vialetto, E. (1936) Contributo alla forma ereditaria della paralisi bulbare progressive. *Riv. Sper. Freniat.*, **40**, 1–24.
- Van Laere, J. (1977) Un nouveau cas de paralysie bulbo-pon-tine chronique progressive avec surdit e. *Rev. Neurol.*, **133**, 119–124.
- Sathasivam, S. (2008) Brown-Vialetto-Van Laere syndrome. *Orphanet. J. Rare. Dis.*, **3**, 9.
- Green, P., Wiseman, M., Crow, Y.J., Houlden, H., Riphagen, S., Lin, J.-P., Raymond, F.L., Childs, A.-M., Sheridan, E. and Edwards, S. (2010) Brown-Vialetto-Van Laere syndrome, a Ponto-Bulbar Palsy with deafness, is caused by mutations in C20orf54. *Am. J. Hum. Genet.*, **86**, 485–489.
- Johnson, J.O., Gibbs, J.R., Van Maldergem, L., Houlden, H. and Singleton, A.B. (2010) Exome sequencing in Brown-Vialetto-van Laere syndrome. *Am. J. Hum. Genet.*, **87**, 567.
- Bosch, A.M., Abeling, N.G., IJst, L., Knoester, H., van der Pol, W. L., Stroomer, A.E., Wanders, R.J., Visser, G., Wijburg, F.A. and Duran, M. (2011) Brown-Vialetto-Van Laere and Fazio Londe syndrome is associated with a riboflavin transporter defect mimicking mild MADD, a new inborn error of metabolism with potential treatment. *J. Inherit. Metab. Dis.*, **34**, 159–164.
- Dezfouli, M.A., Yadegari, S., Nafissi, S. and Elahi, E. (2012) Four novel C20orf54 mutations identified in Brown-Vialetto-Van Laere syndrome patients. *J. Hum. Genet.*, **57**, 613–617.
- Nabokina, S.M., Subramanian, V.S. and Said, H.M. (2012) Effect of clinical mutations on functionality of the human riboflavin transporter-2 (hRFT-2). *Mol. Genet. Metab.*, **105**, 652–657.
- Bandettinidi Poggio, M., Gagliardi, S., Pardini, M., Marchioni, E., Monti Bragadin, M., Reni, L., Doria-Lamba, L., Roccatagliata, L., Ceroni, M., Schenone, A. et al. (2013) A novel compound heterozygous mutation of C20orf54 gene associated with Brown-Vialetto-Van Laere syndrome in an Italian family. *Eur. J. Neurol.*, **20**, e94–e95.
- Koy, A., Pillekamp, F., Hoehn, T., Waterham, H., Klee, D., Mayatepek, E. and Assmann, B. (2012) Brown-Vialetto-Van Laere syndrome, a riboflavin-unresponsive patient with a novel mutation in the C20orf54 gene. *Pediatr. Neurol.*, **46**, 407–409.
- Ciccolella, M., Corti, S., Catteruccia, M., Petrini, S., Tozzi, G., Rizza, T., Carrozzo, R., Nizzardo, M., Bordoni, A., Ronchi, D. et al. (2013) Riboflavin transporter 3 involvement in infantile Brown-Vialetto-Van Laere disease, two novel mutations. *J. Med. Genet.*, **50**, 104–107.
- Haack, T.B., Makowski, C., Yao, Y., Graf, E., Hempel, M., Wieland, T., Tauer, U., Ahting, U., Mayr, J.A. and Freisinger, P. (2012) Impaired riboflavin transport due to missense mutations in SLC52A2 causes Brown-Vialetto-Van Laere syndrome. *J. Inherit. Metab. Dis.*, **35**, 943–948.
- Foley, A.R., Menezes, M.P., Pandraud, A., Gonzalez, M.A., Al-Odaib, A., Abrams, A.J., Sugano, K., Yonezawa, A., Manzur, A.Y., Burns, J. et al. (2014) Treatable childhood neuronopathy caused by mutations in riboflavin transporter RFVT2. *Brain*, **137**, 44–56.
- Anand, G., Hasan, N., Jayapal, S., Huma, Z., Ali, T., Hull, J., Blair, E., Mcshane, T. and Jayawant, S. (2012) Early use of high-dose riboflavin in a case of Brown-Vialetto-Van Laere syndrome. *Dev. Med. Child. Neurol.*, **54**, 187–189.
- Yamamoto, S., Inoue, K., Ohta, K.-Y., Fukatsu, R., Maeda, J.-Y., Yoshida, Y. and Yuasa, H. (2009) Identification and functional characterization of rat riboflavin transporter 2. *J. Biochem.*, **145**, 437–443.
- Yonezawa, A. and Inui, K. (2013) Novel riboflavin transporter family RFVT/SLC52, identification, nomenclature, functional characterization and genetic diseases of RFVT/SLC52. *Mol. Aspects Med.*, **34**, 693–701.
- Ying, Q.-L., Nichols, J., Chambers, I. and Smith, A. (2003) BMP induction of Id proteins suppresses differentiation and sustains embryonic stem cell self-renewal in collaboration with STAT3. *Cell*, **115**, 281–292.
- Ying, Q.-L., Wray, J., Nichols, J., Batlle-Morera, L., Doble, B., Woodgett, J., Cohen, P. and Smith, A. (2008) The ground state of embryonic stem cell self-renewal. *Nature*, **453**, 519–523.
- Wichterle, H., Lieberam, I., Porter, J.A. and Jessell, T.M. (2002) Directed differentiation of embryonic stem cells into motor neurons. *Cell*, **110**, 385–397.
- Hino, S., Sakamoto, A., Nagaoka, K., Anan, K., Wang, Y., Mimasu, S., Umehara, T., Yokoyama, S., Kosai, K. and Nakao, M. (2012) FAD-dependent lysine-specific demethylase-1 regulates cellular energy expenditure. *Nat. Commun.*, **3**, 758.
- Subramanian, V.S., Rapp, L., Marchant, J.S. and Said, H.M. (2011) Role of cysteine residues in cell surface expression of the human riboflavin transporter-2 (hRFT2) in intestinal epithelial cells. *Am. J. Physiol. Gastrointest. Liver Physiol.*, **301**, G100–G109.
- Ho, G., Yonezawa, A., Masuda, S., Inui, K., Sim, K.G., Carpenter, K., Olsen, R.K., Mitchell, J.J., Rhead, W.J. and Peters, G. (2011) Maternal riboflavin deficiency, resulting in transient neonatal-onset glutaric aciduria Type 2, is caused by a microdeletion in the riboflavin transporter gene GPR172B. *Hum. Mutat.*, **32**, E1976–E1984.
- Di Giorgio, F.P., Carrasco, M.A., Siao, M.C., Maniatis, T. and Eggan, K. (2007) Non-cell autonomous effect of glia on motor neurons in an embryonic stem cell-based ALS model. *Nat. Neurosci.*, **10**, 608–614.